Neutron and Gamma Physics Problems in Fusion Reactors

C.W. Maynard and M.A. Abdou

July 1972

UWFDM-17

FUSION TECHNOLOGY INSTITUTE

UNIVERSITY OF WISCONSIN

MADISON WISCONSIN

Neutron and Gamma Physics Problems in Fusion Reactors

C.W. Maynard and M.A. Abdou

Fusion Technology Institute
University of Wisconsin
1500 Engineering Drive
Madison, WI 53706

http://fti.neep.wisc.edu

July 1972

UWFDM-17

NEUTRON AND GAMMA PHYSICS PROBLEMS IN FUSION REACTORS

by

C.W. Maynard and M.A. Abdou

July 1972

FDM 17

University of Wisconsin

Nuclear Engineering Department

NEUTRON AND GAMMA PHYSICS PROBLEMS IN FUSION REACTORS

C.W. Maynard and M.A. Abdou
University of Wisconsin

Introduction

The discussions and results presented here apply to a fusion reactor classified as a D-T fueled low β torodial system. However, most of the paper will apply almost equally well to other systems for the reasons given below.

Fusion reactors may use inertial confinement in the case of laser induced heating or one of several magnetic confinement schemes. While these devices may be very different in many respects, the neutronics and photonics problems associated with them are very similar. In fact, the problems are not very different for different fuel cycles as has been shown by Forsen and McAlees (1). The basic reason for this is that D-T produced neutrons are most important. This is true because at lower plasma temperatures the D-T fusion cross section is larger and a D-T system will operate on this reaction. Even in a D-D or D-He^3 plasma, since tritium is produced in approximately half of the D-D reactions and because of the larger D-T cross section quickly results in a D-T reaction. Since the resulting 14 MeV neutrons carry most of the energy and cause most of the physical effects of interest, they dominate the real and computational problems.

A low β torodial reactor will confine the plasma in a torus surrounded by a coolant and lithium bearing region called the blanket and followed by a shield. The magnet coils are outside this and will be superconducting to achieve the large fields required. Various fueling and exhaust ports breach the blanket and shield and coolant passages must pass between magnet windings. Neutron absorptions in lithium provide the tritium production for fuel breeding. The parameter β is the ratio of particle pressure to magnetic field pressure, and for fixed magnetic field limits the plasma operating temperature.

The results of importance for reactor design fall into the following categories. The helium, proton, and atom displacement production rates are important in evaluating radiation damage problems. The (n,2n) reaction rates as well as the Li^6 and Li^7 tritium production rates influence the tritium breeding ratio. The energy deposition rate by the neutrons and the resulting gammas provide the basic input for heat removal studies. Activation of structural and other materials is important for decay heat and hazards studies; and leakage from the shield determines the heat load to the refrigeration system for the superconducting magnets.

Source Geometry

The monoenergetic neutron source is essentially isotropic because the ions are nearly isotropically distributed and so little of the available momentum of the products is needed to balance the initial momentum that the neutrons would be virtually isotropic regardless of the ion distribution. The source intensity is proportional to the square of the ion density and to the cross section which in the temperature range of interest here is essentially linear in the temperature. The equations governing the spatial distribution of these quantities are the particle and energy conservation equations and the Maxwell equations.

This system of coupled equations can only be solved numerically or by rather drastic simplifying assumptions. For example; if the ion and electron temperatures are assumed to be constant, a uniform ion source is provided, and the ion density is required to go to zero at an arbitrary point short of the actual first wall a parabolic neutron source results for slab and cylindrical geometry for a particle diffusion coefficient proportional to the ion density as expected in the neo-classical diffusion regime. If under the same conditions the diffusion coefficient is constant as in Bohm diffusion, the neutron source is the square of a parabola. In the case of a torus, the source under similar conditions would change from a radial dependence going as the radius squared to a five halves power if one uses the equations of Rosenbluth, Hazeltine and Hinton (2) and makes the further assumption that the poloidal field is linear in the radius. Thus, these plausible sources take the form

$$S(r) = S_o \left[1-\left(\frac{r}{r_p}\right)^{\alpha}\right]^{\beta}$$

where α is two for slabs and cylinders and 5/2 for toroidal geometry and β is one for neo-classical and two for Bohm diffusion. The radius r_p at which the ion density and neutron source become zero is to be fixed by a system of magnet windings which divert any ions beyond this radius out of the central toroidal region. This can also be accomplished conceptually by a cold gas blanket. In any event, from the point of view of the neutron source r_p is a parameter. The results are somewhat sensitive to the ratio of the plasma to wall radii, but fortunately, as will be demonstrated later, the results depend more on the geometry than on the exact distribution and it suffices to use something resembling a parabola.

The high energy of the source neutrons and the resulting scattering anisotropy and energy range of importance imply the need for a multigroup transport treatment of the neutron as well as the gamma flux. At least for survey studies, this means one space variable models such as infinite slabs or cylinders are necessary. However, slab geometry is not acceptable. This is mainly due to the importance of the results in and near the first wall. The reason slab geometry gives poor results can be seen intuitively from the fact that the results are independent of the spatial distribution and the angular distribution incident on the first wall becomes infinite as the angle of incidence approaches a parallel to the wall. In a cylinder with the source not extending to the wall, there are no incident neutrons at right angles to the normal except in the vertical direction and the spatial distribution further increases the tendency to normal incidence. This difference in the geometries causes the slab results to be much too high as illustrated in Table I which is an abreviated form of the results given by the authors earlier (3). The effect of the plasma and wall radii is shown in Table II. As expected from the earlier results, the smaller the ratio r_p/r_w, the smaller the reaction rates in the first few zones and the larger the leakage.

These calculations and others to be given below are based on a standard fusion reactor blanket model adopted for benchmark studies by an ad hoc committee on benchmark and cross sections formed at the International Working Session's on Fusion Reactor Technology held at Oak Ridge in June 1971. The standard blanket is shown schematically in Figure I and a more complete description is given in the Proceedings of the Working Sessions (4). The quantities presented in the table are based on ENDF II data as represented by DLC2 multigroup cross sections and are both important and representative of the trends of the various other quantities required. The calculations were carried out using the discrete ordinates program ANISN (5) and make a six group determination of the neutron flux, reaction rates, and heating for neutrons with energies from 8 to 14.1 MeV. The energy range was chosen to reduce costs while still including most reactions of interst here. It is not readily possible to carry out calculations in toroidal geometry and that would likely be too expensive for most purposes. The cylindrical results should be close to the toroidal and

slightly conservative for essentially the same reasons that slab calculations overestimate results in the first few regions.

Neutronics Calculations Model

The next problems posed are the order required of the transport approximation and the scattering anisotropy. A series of calculations were carried out for a uniform source with a 1.5 meter plasma radius and a two meter wall radius with the results shown in Table III. As the order of approximation is increased the flux anisotropy is treated more adequately and it becomes more forward peaked resulting in decreased reactions in the first zones. However, convergence is adequate by S_6 which is almost as good as S_8 but is not given on this table as it was carried out with a different mesh spacing. The slab reaction rates are again far too high, but interestingly move further from the cylinder results with increasing order of the approximation which means the slab model is even worse than was indicated earlier. Effects of scattering anisotropy are illustrated in Table IV. The calculations are for the same problem used in obtaining Table III and are carried out in S_{16}. Increasing the order of anisotropy retained in the scattering increases the streaming tendency and lowers the heating and reactions in the first wall with convergences achieved by P_3.

Studies were also carried out as to adequate mesh spacing and conformed to a rule that an adequate mesh resulted if the steps were $1/\Sigma_T N$ where N is the order of S_N used and Σ_T is the largest total cross section in any group. The calculations in groups corresponding to lower energies could be performed in lower approximations if convenient without degradation of the quality of the quality of the neutronics results.

Gamma Calculational Model

The gamma flux was also treated using ANISN with a 21 energy group structure. The inital survey of the effects of scattering anisotropy was done in slab geometry for economy using S_{16}. Convergence is not greatly effected by geometry. The results of interest are the heating rate by the gamma flux and the gamma source is obtained from earlier neutron flux results and gamma production cross sections. The boundary condition or albedo is reflecting in this series and a set of results in selected blanket regions for anisotropy through P_n with n from zero to seven is shown in Table V. These results are certainly converged by P_3. However in the problem studied here P_1 doesn't give bad results and one strongly suspects that a transport corrected P_0 would be satisfactory. However, the combination of an isotropic and distributed source cause very low order approximations to work well in this instance. Experience with other gamma flux problems indicates that a P_3 treatment would be prudent even though the above results would allow less. The last column gives the P_7 results but with a void boundary condition. The only results that are affected in a major way are near the right boundary as would be expected. Table VI shows the same general results for a void at the right boundary in two lower order S_N calculations for both slab and cylindrical geometries. The S_6 slab results are within 1% of the S_{16} results and compare very favorably with the last column of the preceeding table indicating that S_6 is adequate as is P_3 anisotropy. However, the cylindrical and slab result differ enough even here to require the cylindrical model; further the S_4-P_0 results are inadequate with respect to the leakage and other results near the right boundary.

Blanket Results

With the S_6 angular flux, P_3 anisotropy, cylindrical geometry model established as satisfactory, a set of results is presented for the blanket region in Table VII. The table is normalized to one neutron per cm^2-sec at the first wall. Adding the contribution of the α particle in the plasma, there is a total

energy of 3.53×10^{-12} watts/cm^2 or 22.1 MeV/cm^2-sec associated with this neutron current. The γ-heating contributes 26.4% of the total heating and might be thought of as a minor contribution. However, this is not the case, for the first wall presents the most difficult cooling problem and there the gamma heating dominates the neutron contribution by more than a factor of ten. Much of the α particle energy will wind up as bremsthralung absorbed in the first wall and this will probably dominate the first wall heat load. To further emphasize the first wall problems, one can see that about 30% of all (n,α),(n,p), and (n,2n) reactions occur in the first wall. The breeding ratio of 1.21 is more than adequate due to the short doubling time associated with these systems (6). Other first wall materials may be chosen over niobium and several seem better from a nuclear viewpoint. The tritium breeding ratio predicted under the same circumstances is higher for both molybdenum (1.45) and vanadium (1.52) among other advantages, but more conventional materials properties will dictate this choice.

Shield Discussion

All of the above discussions apply to the blanket region. Very little has been done on the shield region surrounding the blanket. The reason for this is a lack of some key data for the gamma calculations. Neutron calculations can and have been carried out. These are not particularly enlightening since heating rates and gamma fluxes are not available. Since refrigeration costs are extremely high the energy to the magnets should be attenuated by 10^{-6} to 10^{-7} by the blanket and shield. Calculations with neutrons alone, for a shield made up of a layered structure containing two boron carbide, nine stainless steel, three lead, and four borated water regions totaling 17, 18, 21, and 45 cm respectively, gave a neutron current attenuation of 4.9×10^{-6} which should be adequate when coupled with about two orders of magnitude attenuation in the blanket. The 14 MeV neutrons are the most penetrating and thus a characteristic spectrum developes for these deep penetration neutrons.

Data Situation

Gamma results are not given for the shield as gamma production cross sections are available for only a very limited number of elements. This brings us to the discussion of nuclear data problems for fusion reactors. Basically neutron data is available on ENDF files although its adequacy has not been assessed in many cases. Gamma scattering and absorption cross sections are available from the computer program MUG (7) and no obvious problems appear to us. The main difficulties center around the gamma production cross sections and the Kerma factors (energy deposition parameters). Some Kerma factors are available through the efforts of Ritts, Solomito and Steiner (8) for some materials. A computer program has been written by one of the authors to evaluate the Kerm factors directly from ENDF data. The program calculates the Kerma factors for all reactions which contribute. Preliminary results are available and a complete Kerma library will be generated and released soon by the Radiation Shielding Information Center of Oak Ridge. The gamma production cross sections are available from two computer programs. These are POPOP4 (9) and Laphano (10) but Laphano results are based on ENDF gamma files and data is available for only twelve elements. POPOP4 uses its own library which is somewhat more extensive but the accuracy of the data is uncertain. If the gamma production problem is solved, data for fusion work will be generally available. The data will not be adequately evaluated and sensitivity studies have not been completed but are underway at several installations at this time. This availability of these data will allow complete shielding studies and a calculation of energy deposition in the superconducting magnets which are crucial to the refrigeration systems employed with these systems.

Design Problems

Once the data and model are established, there remains the analysis of special problems involving real two and three dimensional systems and the design oriented problem of finding an optimal configuration. Probably the first problem can be overcome at considerable expense by using Monte Carlo flux calculations. This can probably be carried out even in toroidal geometry. With several criteria such as adequate tritrium breeding, sufficient attenuation of the radiation load to the magnets, and limited first wall energy deposition, it may be difficult to decide on definitive criteria for optimization. However, at this time it appears that there is no great difficulty in achieving the technical goals mentioned above and design will be based on economic considerations for the entire system. For example, a wall loading (plant power divided by first wall area) of about one megawatt per square meter is all that can be produced in a low β system because of the plasma physics and this loading is not currently expected to present an unsurmountable cooling or radiation damage problem. The tritium breeding can be achieved according to current estimates by most workers in the field with a blanket one meter or less in thickness and the shielding with about one additional meter of materials. The trade off then becomes one between blanket and shield materials costs against magnet and refrigeration costs. Speculatively, the magnet costs are so high that the best blanket and shield design may be the thinest unit meeting minimal breeding and attenuation criteria without regard to materials cost in this part of the system.

Bibliography

1. H.K. Forsen and D.G. McAlees, Neutron Wall Current and Energy Considerations for Alternate Fusion Fuel Cycles and Reactor Approaches, Fusion Design Memo 9, University of Wisconsin, Madison, Wisconsin, February 1972.

2. M.N. Rosenbluth, R.D. Hazeltine and F.L. Hinton, Plasma Transport in Toroidal Confinement Systems, Phy. Fluids 15, 116 (1972).

3. M.A. Abdou and C.W. Maynard, Neutron Source Geometry Effects on Fusion Reactor Blankets, Trans. Am. Nuc. Soc., 15, 34 (June 1972).

4. S. Blow and D. Steiner, Summary of Neutronics Session, Proceedings of the International Working Sessions on Fusion Reactor Technology 772, (June 1971).

5. W.W. Engle, Jr., A. Useis Manual for ANISN, K-1693, Oak Ridge Gaseous Diffusion Plant (1967).

6. W.F. Vogelsang, Breeding Ratio, Inventory, and Doubling Time in a D-T Fusion Reactor, Nuclear Technology, to be published.

7. J.R. Knight and F.R. Mynett, MUG; A Program for Generating Multigroup Photon Cross Sections, CTC-17 (Jan. 1970).

8. J.J. Ritts, M. Solomito, and D. Steiner, Kerma Factors and Secondary Gamma-Ray Sources for Some Elements of Interest in Thermonuclera Blanket Assem Assemblies, ORNL-TM-2564 (June 1970).

9. W.E. Ford III and D.H. Wallace, POPOP4: A Code For Converting Gamma-Ray Spectra to Secondary Gamma Ray Production Cross Sections, CTC-12 (May 1969).

10. D.J. Dudziak, R.E. Seamon, and D.V. Susco, LAPHANO: A P_0 Multigroup Photon - Production Matrix and Source Code for ENDF, LA-4750 (ENDF-156), Los Alamos Scientific Laboratory (1972).

SCHEMATIC OF STANDARD BLANKET

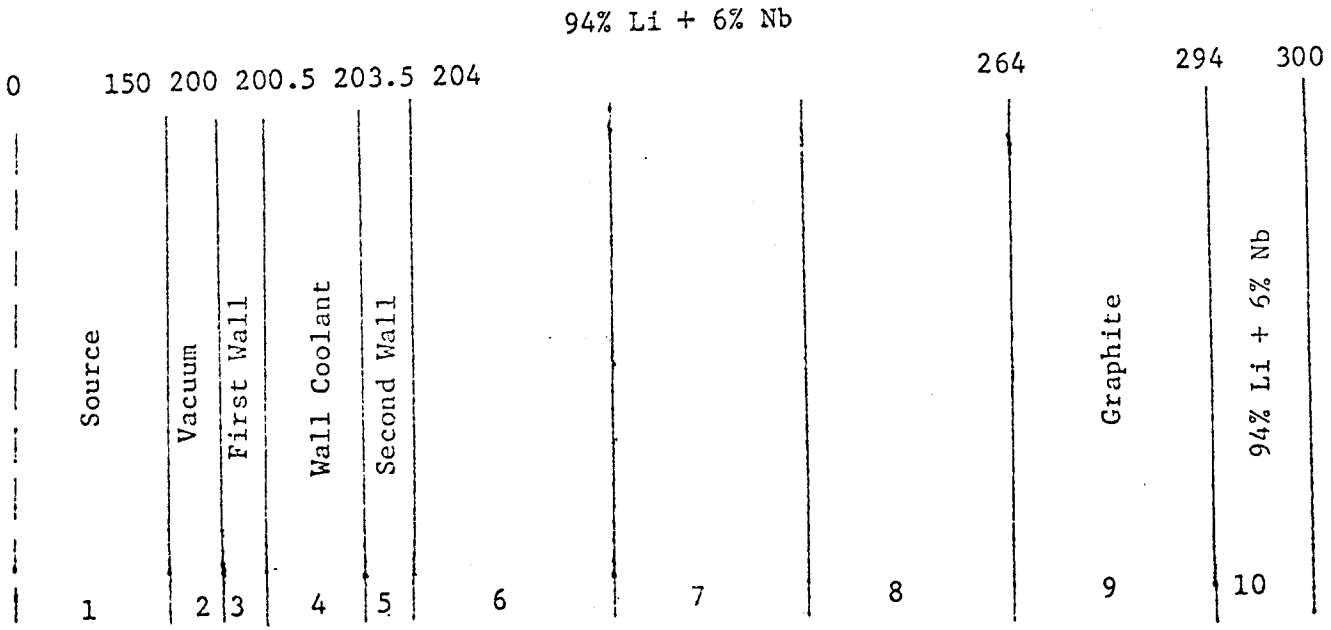

Figure 1

Table I NEUTRON SOURCE GEOMETRY RESULTS

Results Normalized to Unit Current Density

Geometry Source	Zone	Cylinder Volumetric $(\text{Parabolic})^2$	Cylinder Volumetric Uniform	Cylinder Line Isotropic	Slab Volumetric Uniform	Slab Shell Isotropic
Niobium	3	4.42	4.56	3.57	7.77	5.27
$(n,\alpha) \times 10^4$	5	3.01	3.09	2.77	3.68	3.32
	T[a]	15.01	15.21	14.1	18.4	16.02
Neutron	3	0.81	0.83	0.65	1.41	0.96
Heating	4	15.78	16.27	13.77	22.84	18.07
Rate in	5	0.55	0.57	0.51	0.675	0.61
watts $\times 10^{14}$	T[b]	95.95	95.58	97.94	87.62	94.07
Leakage $\times 10^4$	T[c]	37.8	34.4	43.3	17.5	26.1

a. Sum over all zones (for neutrons above 8 Mev)
b. Sum over breeding zones (for neutrons above 8 Mev)
c. Sum for neutrons above 8 Mev (assuming no reflection)

Table II

Neutronics Results for Uniform Source to the Plasma

(Results Normalized to Unit Current Density)

Wall Radius r_w (meters)	Zone	2	2	2	8
Plasma Radius r_p (meters)		1.5	.1	line source	7.5
Niobium $(n,\alpha) \times 10^4$	3	4.56	4.33	3.57	4.92
	5	3.09	2.95	2.77	3.24
	T[a]	15.2	14.8	14.1	15.6
Neutron Heating Rate in watts $\times 10^{14}$	3	0.83	0.79	0.65	0.89
	4	16.3	15.5	13.8	17.3
	5	0.57	0.54	0.51	0.59
	T[b]	95.6	96.1	97.9	94.9
Leakage $\times 10^4$	T[c]	34.4	38.3	43.3	28.2

a. sum over all zones (for neutrons above 8 MeV)

b. sum over breeding zones (for neutrons above 8 MeV)

c. sum for neutrons above 8 MeV (assuming no reflection)

Table III Order of Approximation

S_N Order and Geometry	zone	Cylinder S_4	Cylinder S_8	Cylinder S_{12}	Cylinder S_{16}	Slab S_4	Slab S_8	Slab S_{16}
Result								
Niobium $(n,\alpha) \times 10^4$	3	4.82	4.61	4.57	4.55	6.15	7.77	8.18
	5	3.32	3.14	3.10	3.08	3.93	3.68	3.55
	T[a]	15.59	15.28	15.21	15.18			
Neutron Heating Rate $\times 10^{14}$ (watts)	3	0.879	0.841	0.833	0.830	1.12	1.42	1.49
	4	17.5	16.5	16.3	16.2	21.5	22.8	22.4
	5	0.608	0.576	0.567	0.565	0.720	0.675	0.650
	T[b]	98.3	99.3	99.5	99.5	94.4	96.8	95.3
Leakage $\times 10^4$	T[c]	36.9	33.8	34.3	34.4	18.0	17.6	17.6

a. Sum over all zones (for neutrons above 8 MeV)
b. Sum over breeding zones (for neutrons above 8 MeV)
c. Sum for neutrons above 8 MeV (assuming no reflection)

Table IV SCATTERING ANISOTROPY

(Order of P_n)

Scattering Order	zone	P_0	P_1	P_2	P_3	P_4	P_5
Niobium $(n,\alpha) \times 10^4$	3	6.01	4.57	4.56	4.55	4.55	4.54
	5	3.84	3.14	3.07	3.08	3.08	3.08
	T[a]	17.20	15.30	15.20	15.20	15.25	15.20
Heating Rate $\times 10^{14}$ (watts)	3	1.10	0.834	0.832	0.830	0.830	0.828
	4	21.00	16.30	16.10	16.20	16.20	16.20
	5	0.704	0.575	0.562	0.565	0.564	0.565
	T[b]	95.50	99.70	99.60	99.50	99.50	99.60
Leakage $\times 10^4$	T[c]	3.87	22.70	33.40	34.40	34.30	34.30

a. Sum over all zones (for neutrons above 8 MeV)
b. Sum over breeding zones (for neutrons above 8 MeV)
c. Sum for neutrons above 8 MeV (assuming no reflection)

Table V Gamma Scattering Anisotropy Convergence

21 energy groups, slab S_{16}, 1 photon/sec

Order of P_n Zone	P_0	P_1	P_2	P_3	P_4	P_6	P_7	P_7 [a]
3 [b]	8.0597	7.9087	7.9432	7.9297	7.9342	7.9324	7.9316	7.9240
4	2.7702	2.7180	2.7297	2.7257	2.7271	2.7268	2.7267	2.7238
5	7.0977	6.9699	6.9960	6.9876	6.9902	6.9895	6.9894	6.9814
6	12.0342	11.874	11.8916	11.8923	11.8906	11.8917	11.8925	11.8686
7	6.0468	6.0767	6.0542	6.0656	6.0615	6.0626	6.0627	6.0245
8	3.0105	3.1059	3.0828	3.0894	3.0885	3.0886	3.0885	3.0184
9	2.5544	2.9073	2.8667	2.8695	2.8697	2.8695	2.8695	2.3770
10	0.2470	0.2868	0.2903	0.2884	0.2888	0.2886	0.2886	0.1398
L [c]	1.1515	1.5254	1.5742	1.5648	1.5670	1.5665	1.5664	1.2543

a. All cases except this carried out with a reflecting boundary condition on the right, while here a void condition is used.

b. Heating rates in niobium (zones 3-9) and graphite (zone 10) are in watts x 10^{15}

c. Right boundary positive current x 10^3

Table VI Slab - Cylinder Comparison

For Gamma Transport Calculation

Order of Approximation	S_6, P_3		S_4, P_0	
Zone/Geometry	Cylinder	Slab	Cylinder	Slab
3[a]	7.25828	7.80623	7.36158	7.83919
4 (Nb)	2.53098	2.69892	2.57156	2.71759
4 (Li)	0.73625	0.78866	0.760072	0.80484
5	6.58181	6.95842	6.69689	7.03164
10	2.73871	2.36319	2.46407	2.12604
L[b]	1.57105	1.25367	1.03650	0.81425

a. Heating rates in watts x 10^{15}

b. Right boundary leakage x 10^{3}

Table VII Summary of Blanket
Neutronic and Photonic Results
Cylinderical Geometry - $S_6 - P_3$

Zone	3	4	5	6+7+8	9	10	Sum over all zones
$Nb(n,\alpha) \times 10^4$	4.66	1.39	3.23	6.27	-	0.008	15.56
$Nb(n,p) \times 10^4$	15.48	4.66	10.92	22.09	-	0.03	53.18
Nb dpa $\times 10^{21}$	9.25	8.14	7.06	2.23	-	0.039	
neutron heating[a]	0.97	27.2	0.662	168.00	4.38	3.25	204.26
gamma heating	14.10	6.47	12.81	54.10	5.30	0.445	93.23
$Nb(n,2n) \times 10^2$	2.204	0.654	1.510	2.822	-	0.003	7.19
$Li^7(n,\alpha n')T$	-	0.07	-	0.384	-	0.0007	0.46
$Li^6(n,\alpha)T$	-	0.04	-	0.686	-	0.0197	0.75
neutron leakage							0.032
gamma leakage							0.023

a. Neutron, gamma and total heating rates are in watts $\times 10^{14}$